Influence of Intrinsic Parameters over Extrinsic Calibration between a Multi-Layer Lidar and a Camera

Sergio Alberto Rodriguez Florez, Vincent Fremont, Philippe Bonnifait

Influence of Intrinsic Parameters over Extrinsic Calibration between a Multi-Layer Lidar and a Camera

Sergio A. Rodriguez F., Vincent Frémont and Philippe Bonnifait

Abstract— **In this paper, we present an extensive study about the influence and the behavior of the intrinsic camera calibration imprecisions and their propagation into the extrinsic calibration between a camera and a multi-layer lidar. Usually, the extrinsic calibration process involves the pose estimation of a reference object in the Cartesian frame of each sensor. From this fact, it is necessary to know the camera intrinsic parameters for estimating the position of an object on an image. Therefore, the extrinsic calibration process is directly dependent of the intrinsic camera parameters. By using different projective camera models, we estimate the influence with respect to the computation of the extrinsic parameters.**

Keywords: Multi-sensor system, Extrinsic Calibration, Circle based calibration target

I. INTRODUCTION

In the framework of multi-sensor fusion and object detection, an important aspect is the consistency and the quality of the merged information. Occasionally, in the case of sensors like camera and lidar, the information exchange is mainly geometric. In this case, the consistency of this information exchange depends on the extrinsic parameters (i.e. rigid transformation) which relate them. The extrinsic parameters are generally estimated using the measures reported by the sensors. From this fact, the calibration procedure consists in estimating the rigid transformation between a common set of measurements which minimizes the transformation error. Accordingly, the precision in the set of measurements to be used in this process is critical, especially if there is a large relative distance between the sensors like in vehicular applications (see Figure 1).

Previous works on extrinsic laser-camera calibration solve with accuracy the rigid transformation between a CCD camera and a one-row laser range-finder [1] [2]. Another calibration approach for outdoor scan systems without using a calibration target is presented in [3]. However, the assumptions on the projective camera model and the errors in the estimation of the intrinsic parameters can lead to a 3D biased perception. This work shows how the intrinsic parameters of the camera influence on the estimate of the rigid transformation between a camera and a multi-layer lidar.

This paper is outlined as follows. Section II presents the multi-sensor system, the extrinsic calibration problem, the mathematical models, the theoretical basis and definitions. In section III, we present the calibration method summarized in a circle-based target pose estimation step and rigid transformation computation step. Then, the calibration algorithm summary is clarified in section IV. Finally, results obtained using two different camera projective models with simulated data and real acquisitions are presented in section V.

Manuscript received Juin 11, 2008. Sergio A. Rodriguez F., Vincent Frémont and Phillipe Bonnifait are with Heudiasyc UMR CNRS 6599, Université de Technologie de Compiègne, BP20529 - 60205 Compiègne Cedex, France. Emails: srodrigu@hds.utc.fr,vincent.fremont@hds.utc.fr, and philippe.bonnifait@utc.fr

II. MULTI-SENSOR SYSTEM

The multi-sensor system is rigidly fixed to the vehicle and composed of a multi-layer range finder and a CCD camera. The multi-layer lidar is located in the bumper section and the camera is placed behind the windshield (see Figure 1). This positioning only presents some occlusions to the camera for short distances with respect to the multi-layer range finder.

A. Problem Statement

The problem consists in calculating the rigid transformation (6 dof corresponding to a rotation matrix and a translation vector) between the camera and the 4-layer lidar frames. In order to obtain an accurate estimation of the extrinsic parameters, we use a method which takes advantage of photographic and laser range data by using a circle-based calibration target. It is worth to mention that the laser beam of the lidar sensor is invisible (see Figure 1). The circle-based calibration target is a rigid plane with a printed black ring. The inner circle of the black ring describes a plane perforation. The following are the advantages of using the proposed calibration target. Firstly, it allows to obtain an accurately estimation of the pose in the lidar frame. It is possible by computing a circle fitting in the 3D space of the lidar impacts lying in the contour of the perforation border in the calibration target. Secondly, the geometric and algebraic constraints of the two concentric circles generated by the black ring, and their image projection allow us to obtain a simultaneous estimation of the camera pose and the intrinsic parameters (i.e. the focal lengths and the principal point).

B. Sensor Models and Frames

Our multi-layer lidar model is composed of 4 crossed-scan-planes with a layer relative altitude aperture of 0.8° and a constant azimuthal angle resolution. Figure 2 illustrates, in a general way, the emission direction of the laser layers.

Let be i the layer ID and j the scan point element. Thus, a 3D laser impact is defined in the lidar frame, l, as:

$$ {}^{l}\mathsf{P}_{ij} = \left[\begin{array}{ccc} {}^{l}P_x, & {}^{l}P_y, & {}^{l}P_z \end{array} \right]^T \tag{1} $$

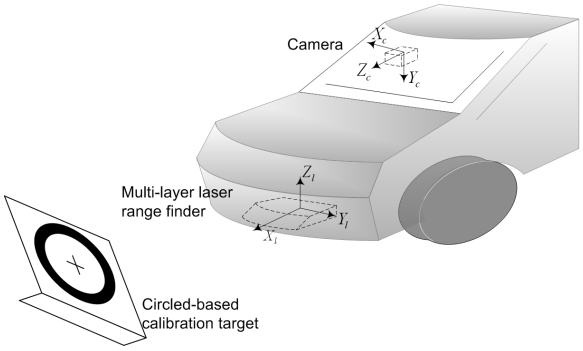

Fig. 1. Overview of the proposed strategy (the lidar is often significantly located far away from the camera)

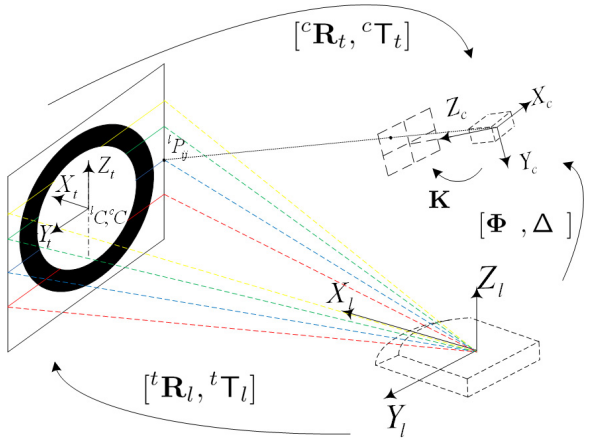

Fig. 2. Rigid transformations

At this point, let us consider the complete multi-sensor model where the data provided by the lidar and the camera are related by using a common detected object (i.e. circle-based calibration target). We proceed to formalize the lidar to camera transformation as a composition of the partial rigid transformations illustrated in the Figure 2. Therefore, the rigid transformation of a 3D point in the lidar frame, ${}^l\mathsf{P}_{ij}$, into the camera frame is given by the following equation:

$$ {}^c\mathsf{P}_{ij} = {}^c\mathbf{R}_t \cdot ({}^t\mathbf{R}_l \cdot {}^l\mathsf{P}_{ij} + {}^t\mathsf{T}_l) + {}^c\mathsf{T}_t \tag{2} $$

simplifying,

$$ {}^c\mathsf{P}_{ij} = \mathbf{\Phi} \cdot {}^l\mathsf{P}_{ij} + \Delta \tag{3} $$

with $\mathbf{\Phi} = {}^c\mathbf{R}_t \cdot {}^t\mathbf{R}_l$ and $\Delta = {}^c\mathbf{R}_t \cdot {}^t\mathsf{T}_l + {}^c\mathsf{T}_t$ respectively the orientation and the position of the lidar sensor with respect to the camera. The rigid transformation composed of $[\mathbf{\Phi}, \Delta]$ are the unknown values of the calibration problem.
Additionally, the impact location of the lidar measurements can be projected into the image even if the lidar beam is invisible. For this purpose, the equation (3) and a classical pinhole model are considered. Hence, the image projection of a 3D point in the camera frame, ${}^c\mathsf{P}_{ij}$, is given by

$$ [p_x,\ p_y,\ 1]^T \sim \mathbf{K} \cdot {}^c\mathsf{P}_{ij} \tag{4} $$

with

$$ \mathbf{K} = \begin{pmatrix} f_x & 0 & u_0 \\ 0 & f_y & v_0 \\ 0 & 0 & 1 \end{pmatrix} \tag{5} $$

where $\mathbf{K}$ is the intrinsic calibration matrix with f_x and f_y the focal distance in x and y direction of the camera in pixels units and $[u_0,\ v_0]^T$ the image coordinates of the principal point, assuming no distortion and zero skew. The operator $\sim$ denotes "up to a scale factor". Finally, the image projection of ${}^l\mathsf{P}_{ij}$ is computed by replacing the equation (3) in (4):

$$ [p_x,\ p_y,\ 1]^T \sim \mathbf{K} \cdot (\mathbf{\Phi} \cdot {}^l\mathsf{P}_{ij} + \Delta) \tag{6} $$

III. EXTRINSIC CALIBRATION

The method employed for obtaining the extrinsic parameters consists in estimating different poses of the calibration object detected simultaneously by the camera and the multi-layer lidar. A minimum of 6 poses [4] have to be estimated in the lidar and the camera frame in order to get all degrees of freedom. Each pose of the calibration target is parameterized by the 3D coordinates of the circle center and the normal vector of its plane. Then, a first estimation of the rigid transformation is obtained by solving the usual absolute orientation problem [4]. This solution consists in determining the relationship between the two coordinate frames using sets of corresponded features (i.e. circle centers of each pose). Finally, a non-linear 3D error minimization is done in order to refine the estimated extrinsic parameters.

A. Target pose estimation in the lidar frame

First, a robust detection of the circle in the 3D space is obtained by applying the robust outlier rejection technique proposed in [1] on several 4-layers lidar scans. Then, the points lying in the perforation border of the calibration target are extracted. Taking into account that the pose of target frame origin with respect to the lidar frame is defined by the inversed transformation illustrated in Figure 2 where ${}^t\mathbf{R}_l^T$ corresponds to the orientation of the calibration frame and its origin in the lidar frame, ${}^l\mathsf{C} = -({}^t\mathbf{R}_l^T \cdot {}^t\mathsf{T}_l)$. Based of this fact, we perform a nonlinear 3D circle fitting problem constrained to a known radius, r, and parameterized as follows: $\hat{\alpha}$, $\hat{\beta}$ are orientation angles of the 3D circle axis vector, ${}^l\mathsf{N}(\hat{\alpha}, \hat{\beta})$, with respect to y-axis and z-axis respectively and ${}^l\hat{\mathsf{C}} = [{}^l\hat{C}_x,\ {}^l\hat{C}_y,\ {}^l\hat{C}_z]^T$ are the Cartesian coordinates of the estimated 3D circle center coincident with the target frame origin (see Figure 2). By using the geometric criteria as stated in [5]:

$$ {}_i\Pi_1 = {}^l\mathsf{N}(\hat{\alpha}, \hat{\beta}) \cdot \overrightarrow{{}^l\hat{\mathsf{C}}{}^l\mathsf{P}_i} \tag{7} $$

$$ {}_i\Pi_2 = \| {}^l\mathsf{N}(\hat{\alpha}, \hat{\beta}) \times \overrightarrow{{}^l\hat{\mathsf{C}}{}^l\mathsf{P}_i} \| - r \tag{8} $$

with $\overrightarrow{{}^l\hat{\mathsf{C}}{}^l\mathsf{P}_i} = {}^l\mathsf{P}_i - {}^l\hat{\mathsf{C}}$.

Where:

- ${}_i\Pi_1$ corresponds to the Euclidean distance between a target-contour laser range finder impact, ${}^l\mathsf{P}_i$, and the

3D plane defined by ${}^{l}\mathsf{N}(\hat{\alpha},\hat{\beta})$ and the estimated circle center, ${}^{l}\hat{\mathsf{C}}$.

- ${}_{i}\Pi_2$ represents the Euclidean distance between a target-contour laser range finder point, ${}^{l}\mathsf{P}_i$, and the 3D circle axis defined by ${}^{l}\mathsf{N}(\hat{\alpha},\hat{\beta})$ and the estimated circle center, ${}^{l}\hat{\mathsf{C}}$.

Accordingly, we minimize the geometric criteria (7) and (8) using the Levenberg-Marquardt algorithm (LM-algorithm) [6]. After convergence of the non linear minimization algorithm and by applying this technique to various poses (6 poses are needed for a solution) of the calibration target, we obtain not only a first set of 3D laser features (i.e. circle centers, ${}^{l}\hat{\mathsf{C}}$, and normal plane vectors, ${}^{l}\mathsf{N}$) but also a 3D circle reconstruction in the laser range finder frame for every pose. Now, in order to acquire the corresponded features in the camera frame, we have to analyze the image.

B. Target pose estimation in the camera frame

Like several camera calibration methods using projected concentric circles [7] [8] [9], we estimate the position of the calibration target in the camera frame. For this purpose, it is necessary to estimate the intrinsic camera parameters. As stated in [7], all intrinsic calibration parameters can be obtained first by computing the *image of the absolute conic* (IAC) with precision [10] from the *imaged circular points* [11] [10] from three images of two concentric circles under different orientations. By using the method exposed in [7] the intrinsic camera parameters denoted in (5) are obtained. Let us define A_1 and A_2 as the pixel centered point set of the principal (i.e. external) and secondary (i.e. internal) circle projection which can be obtained by the segmentation methods widely explained in [9] [12]. Achieving a non linear ellipse fitting algorithm stated in [13], we obtain two conic matrices, $\mathbf{Q}_1$ and $\mathbf{Q}_2$, which are defined as follows:

$$\mathbf{Q} = \begin{pmatrix} \mathbf{a}(f_x/f_y) & \mathbf{b}/2 & \mathbf{d}/2f_y \\ \mathbf{b}/2 & \mathbf{c}(f_x/f_y) & \mathbf{e}/2f_x \\ \mathbf{d}/2f_y & \mathbf{e}/2f_x & \mathbf{f}/(f_x f_y) \end{pmatrix} \tag{9}$$

Where $\mathbf{a},\mathbf{b},\mathbf{c},\mathbf{d},\mathbf{e},\mathbf{f}$ are the conic parameters and f_x, f_y are the focal lengths in pixels. $\mathbf{Q}_1$ and $\mathbf{Q}_2$ are normalized to $\det \mathbf{Q} = -1$. Extending the concept presented in [9] to our camera model, the scale uncertainty is removed and the normal vector to the target plane is given by:

$${}^{c}\mathsf{N}_0 = \mathbf{Q}_1 \begin{bmatrix} x_c/f_x \\ y_c/f_y \\ 1 \end{bmatrix} \tag{10}$$

Where x_c and y_c are the image coordinates of the projected circle center. Finally, the 3D circle center in the camera frame, ${}^{c}\hat{\mathsf{C}}$, is obtained as stated in [9]:

$${}^{c}\hat{\mathsf{C}}_0 = \frac{\sqrt{\lambda^3}\ R\ [x_c/f_x\ \ y_c/f_y\ \ 1]^T}{{}^{c}\mathsf{N}_0 \cdot [x_c/f_x\ \ y_c/f_y\ \ 1]^T} \tag{11}$$

Where λ is the smaller positive eigenvalue of Q_1 and R is the radius of the principal circle in the target object. ${}^{c}\mathsf{N}_0$ and ${}^{c}\hat{\mathsf{C}}_0$ represents an algebraic closed-form solution of the camera pose estimation which could be very sensible to noise conditions but usually a very good first estimation. Therefore, an accurate camera pose estimation is obtained by minimizing the conic parameter error obtained between the 3D circle image projection and the image segmented conic,

$$f_{({}^{c}\mathsf{N},||{}^{c}\hat{\mathsf{C}}||)} = \min(\epsilon) \tag{12}$$

with ϵ as the conic parameter error function

$$\epsilon = ||e_x^2 + e_y^2 + e_M^2 + e_m^2 + e_\theta^2|| \tag{13}$$

where e_x, e_y, e_M, e_m and e_θ are the errors of the ellipse center, the major axis, the minor axis and orientation angle respectively. It is worth to mention that the number of the nonlinear minimization parameters is reduced by taking into account the direction of the translation vector, $\overrightarrow{{}^{c}\hat{\mathsf{C}}}$, as an accurate estimation. $\overrightarrow{{}^{c}\hat{\mathsf{C}}}$ is given by the image back-projection of the projected circle center as follows,

$$\overrightarrow{{}^{c}\hat{\mathsf{C}}} = \mathbf{K}^{-1} \begin{bmatrix} x_c \\ y_c \\ 1 \end{bmatrix} \tag{14}$$

The Figure 3 illustrates the algebraic closed-form solution of the camera pose estimation, the nonlinear proposed solution after convergence and the direction of the translation vector.

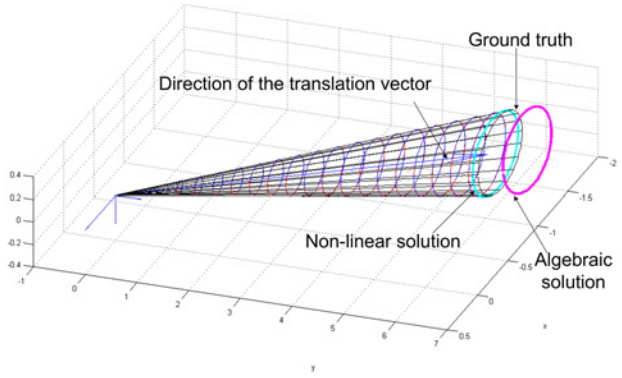

Fig. 3. Example of the camera pose estimation under an image noise of 3 pixels

C. Estimation of the rigid transformation between the lidar and the camera

The method presented in the above subsection allows us estimating the 3D center points of the circle-based calibration target for various poses. These pose estimations are composed with 3D corresponding center point set in the camera and the laser range finder frame. Therefore, in order to estimate an initial guess solution we formulate the extrinsic calibration as a classical absolute orientation problem.

1) Initial guess from a linear solution: A well-known closed-form solution for this problem is the method developed by Arun et al. [14]. This method consists in obtaining the optimal rotation from the singular value decomposition

(SVD) of the correlation matrix of the centered point sets represented by $\mathbf{\Sigma}$:

$$\mathbf{\Sigma}=[{}^{l}\hat{\mathsf{C}}_i - {}^{l}\bar{\mathsf{C}}][{}^{c}\hat{\mathsf{C}}_i - {}^{c}\bar{\mathsf{C}}]^T \quad (15)$$

$$\mathbf{\Sigma}=\mathbf{U}\ \mathbf{S}\ \mathbf{V}^T \quad (16)$$

Where ${}^{l}\hat{\mathsf{C}}_i$ are the coordinates of the 3D-circle center point set estimated from the i^{th} pose by the laser range finder measures, ${}^{l}\bar{\mathsf{C}}$ is the centroid of the 3D-circle center point set in the laser range finder frame,${}^{c}\hat{\mathsf{C}}_i$ are the coordinates of the 3D-circle center point set estimated from the i^{th} pose by the camera measures and ${}^{c}\bar{\mathsf{C}}$ is the centroid of the 3D-circle center point set in the camera frame. Thus, the 3x3 optimal rotation matrix is obtained as follows:

$$\mathbf{\Phi}_0 = \mathbf{V}\mathbf{U}^T \quad (17)$$

The translation, Δ_0, is obtained as the vector which aligns the centroid of the 3D-circle center point set in the camera frame, ${}^{c}\bar{\mathsf{C}}$, and the rotated centroid $\mathbf{\Phi}_0 \cdot {}^{l}\bar{\mathsf{C}}$:

$$\Delta_0 = {}^{c}\bar{\mathsf{C}} - \mathbf{\Phi}_0 \cdot {}^{l}\bar{\mathsf{C}} \quad (18)$$

2) Refining parameters: The rigid transformation obtained in the above section, $[\mathbf{\Phi}_0, \Delta_0]$, is a linear minimization of the Euclidean distance error between the 3D circle center point sets. This solution is usually a good starting guess of the extrinsic calibration. Therefore, in the aim of refining these estimated parameters, we first generate the 3D circles of the n poses estimated by the camera. It consists in computing m points of each estimated circle pose by using the 3D circle center and an orthonormal base lying in circle's plane. This orthonormal base is obtained from the normal vector to the circle's plane applying the *Gram-Schmidt procedure* [15]. Let be ${}^{c}\mathsf{F}_{i,k}$, the k^{th} generated 3D point using the camera estimation of the i^{th} pose. Secondly, the 3D circles of all the poses estimated by the lidar are generated in the same way as presented for the camera estimations obtaining ${}^{l}\mathsf{F}_{i,k}$. Then, we apply systematically the first guess for the rigid transformation, $[\mathbf{\Phi}_0, \Delta_0]$, as in the equation (3). Thirdly, under the assumption that the error orientation of the first guess rigid transformation is lower than $\pi/2$, we match the 3D points of the camera and lidar transformed estimations for every pose by using the nearest neighbor criterion as illustrated in Figure 4. At this point, it is worth to mention that we have a 3D point set of camera and lidar observations associated. Finally, the refining of the rigid transformation parameters, $[\alpha,\ \beta,\ \rho,\ t_x,\ t_y,\ t_z]^T$, is obtained by minimizing the following non-linear objective function:

$$\epsilon = \sum_{i=1}^{n}\sum_{k=1}^{m} \mathbf{W} \cdot [D_{ik}^2] \quad (19)$$

with

$$D_{ik} = ||{}^{c}\mathsf{F}_{i,k} - [\mathbf{\Phi}_{(\alpha,\beta,\rho)} \cdot {}^{l}\mathsf{F}_{i,k} + \Delta_{(t_x,t_y,t_z)}]|| \quad (20)$$

Where D_{ik} represents the Euclidean distance residual of the points after applying the rigid transformation and $\mathbf{W}$ is a weighting matrix. The results are obtained by using a robust M-estimator algorithm for calculating the robust weights as stated in [16] and the LM-algorithm. After convergence, the solution of the calibration problem is represented by $[\mathbf{\Phi}, \Delta]$.

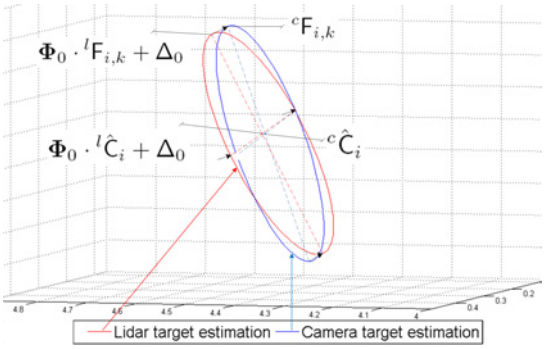

Fig. 4. Matching of the camera and lidar estimations

IV. CALIBRATION ALGORITHM

The following is a summary of the calibration method explained in section III.

Algorithm 1 Circle-based Extrinsic Calibration Technique

1: **for** $i = 1$ to at least 6 **do**
2: Estimate the i_{th} lidar calibration pose, $[{}^{l}\mathsf{N}\ {}^{l}\hat{\mathsf{C}}]_i$, as stated in section III-A
3: Estimate the i_{th} camera calibration pose, $[{}^{c}\mathsf{N}\ {}^{c}\hat{\mathsf{C}}]_i$, as stated in section III-B
4: **end for**
5: Compute a first guess, $[\mathbf{\Phi}_0, \Delta_0]$, for the lidar-camera rigid transformation using the linear solution (III-C.1)
6: Match the 3D circle poses estimations (III-C.2)
7: **repeat**
8: Non-linear minimization using LM-algorithm
9: Robust noise variance estimation σ^2 based in non-linear minimization residuals
10: Weighting matrix $\mathbf{W}$ update from M-estimator
11: **until** convergence of $[\mathbf{\Phi}, \Delta]$

V. EXPERIMENTAL RESULTS

Evaluation tests have been carried out in order to estimate the behavior and robustness of the presented method in simulated and real conditions. They were implemented using Matlab 7.4.

A. Synthetic data

Considering similar conditions to our multi-sensor system, the simulation model correspond to the sensor relative position on board the vehicle. The extrinsic parameters used were the translation vector in meters $\Delta = [-0.2,\ 0.8,\ 1.8]^T$ and the orientation matrix $\mathbf{\Phi}_{\alpha,\beta,\rho}$, computed from the rotation angles $\alpha = 11°$, $\beta = -1°$ and $\rho = 0.5°$. The multi-layer lidar impacts were generated as the intersection of the lidar beam emission vectors and the simulated calibration target plane. A 3D space constraint

was used to guarantee that all lidar layers impact the calibration object. Then, a Gaussian white noise was added in the direction of the lidar beam emission vector. By using the model presented in (4), a synthetic image was computed as a discrete image projection of the circle-based calibration target. The intrinsic parameters used in the camera model were a focal length in x direction f_x, a focal length in y direction f_y and principal point (u_0, v_0). Next, a Gaussian white noise was added to the image projection coordinates of the circle-based calibration target and to the intrinsic parameters of camera model.

1) Test No. 1: A first Monte Carlo-like simulation test was made in order to evaluate the behavior of the extrinsic calibration method with regard to the intrinsic parameters of the camera. Thus, 7 random poses were oriented randomly in the common field of view (FOV) of the multi-sensor system by 50 trials. A Gaussian-white noise in a range between 1 to 3 pixels of standard deviation, σ_b, was added to the image coordinates. The camera model used for this test was constrained to an unitary aspect ratio. For each trial, the extrinsic parameters were estimated. The results obtained by the robust non-linear minimization of the 3D poses (see III-C) are presented in the Figure 5(a) and 5(b). We have also executed an iterative closest point algorithm (ICP) [18] as a reference of a classical registration of 3D point sets.

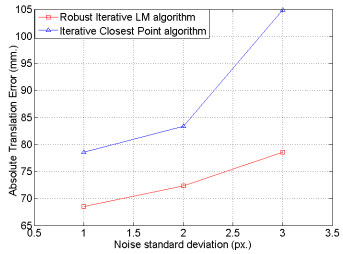

(a)

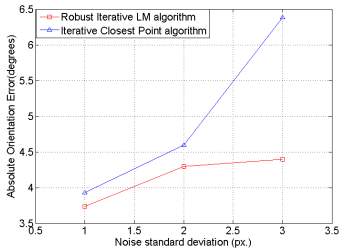

(b)

Fig. 5. Absolute errors using camera model with unitary aspect: (a) Translational (mm.); (b) Orientation (degrees)

2) Test No. 2: A second test was performed taking into account the same conditions used for test No. 1 but now the camera model was unconstrained to a non-unitary aspect ratio. This test let us estimate the influence of the camera model over the absolute error of the extrinsic calibration parameters. Figure 6(a) and 6(b) illustrate an important improvement by using an unconstrained camera model.

The results obtained in the test No.1 and No.2 reveal that the intrinsic parameters have an important influence over the

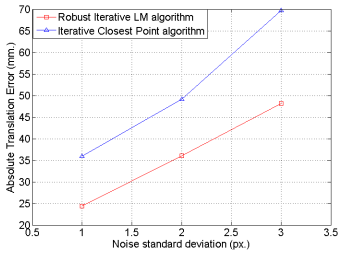

(a)

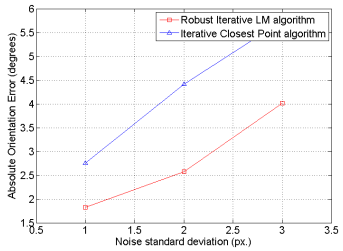

(b)

Fig. 6. Absolute errors using unconstrained camera model: (a) Translational (mm.); (b) Orientation (degrees)

extrinsic parameters. Let recall that the extrinsic calibration method is based only in the minimization of the euclidean error between the lidar and the camera perception.

B. Real data

Experiments using real data were made thanks to the experimental platform of the Heudiasyc laboratory (see Figure 7(a)). This vehicle is equipped with an IBEO Alasca XT and a camera Sony DFW-VL500. The resolution of the camera was set to 640×480 pixels. We have used a calibration target with 2 concentric circles of radii 33 cm and 23 cm. The camera focal distances f_x and f_y have been estimated by using the circle-based calibration target. However, the principal point was estimated by using the classical Zhang's method [19] due aux some instabilities observed under these experimental conditions (i.e. the important distance of the calibration target with respect to the camera). A number of 20 scans were taken into account for each pose in the calibration process. Only 7 poses were used to estimate the initial guess solution for the rigid transformation. By using the rigid transformation,

Fig. 7. Experimental platform: Lidar (left), Camera (right)

a projection of the multi-layer measurements into the scene image was made and illustrated in Figure 8 and Figure 9. The image projection of the lidar data reveals that the error induced by the assumption of unitary aspect ratio in the projective camera model are almost imperceptible but the table I shows that the assumption provides an estimate of the

Results of the Test using Real Data			
Translation	Two-Focal Camera	One-Focal Camera	Measured
tx	-0.1651 m	-0.3331 m	-0.2 m
ty	0.9208 m	0.9246 m	0.88 m
tz	1.8466 m	1.8027 m	1.82 m
Rotation angles			
Rx	1.5370 rad	1.5428 rad	N/A
Ry	-0.0455 rad	-0.0505 rad	N/A
Rz	1.6075 rad	1.6296 rad	N/A

TABLE I

RESULTS ACHIEVED WITH REAL DATA

relative position without which is biased. It is observable by the increase in the absolute error in the previous simulations.

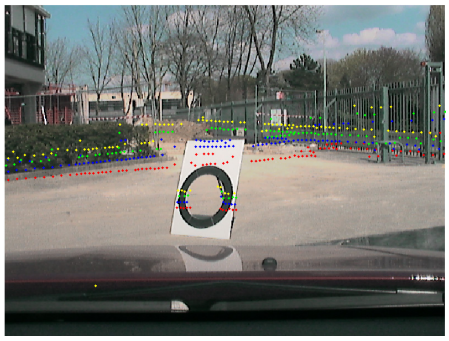

Fig. 8. Projection image of lidar data using the extrinsic calibration method and an unconstrained aspect ratio camera model

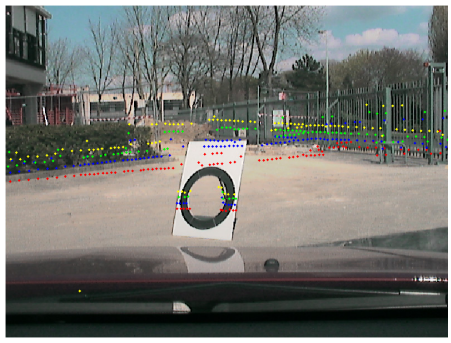

Fig. 9. Projection image of lidar data using the extrinsic calibration method and an unitary aspect ratio camera model

VI. CONCLUSION

By using two different projective camera models, we have shown the influence of the intrinsic parameters over the extrinsic calibration between a multi-layer lidar and a camera. The simulation results show that the intrinsic parameters errors (i.e. focal distance and principal point) have important impact on the extrinsic calibration process: up to 80 mm translation error using a pinhole camera model with unitary aspect ratio, no distortion and zero skew.

For instance, this means that a perception system that detects obstacles using a lidar and then uses a camera for recognition can cope with these errors. Contrary, a 3D data fusion system will be very sensitive to camera intrinsic errors.

Nevertheless, the real experiments have shown that the intrinsic parameters errors are not perceptible in the projection of the lidar data in the image. At this point, it is important to mention that in real conditions, there are some critical points like the lidar imprecisions due to surface's reflectivity and the segmentation errors of the ellipse in the image that have also influence in the performance of the calibration algorithm. These critical points can be one of the reasons why the effects due to the intrinsic parameters of the camera are not quite visible in the experimental results of extrinsic calibration method.

The improvement of the accuracy and the stability of the intrinsic calibration methods based in concentric circles constitutes a perspective of this research, especially for a correct estimation of the principal point.

REFERENCES

[1] R. Dupont, R. Keriven and P. Fuchs, "An improved calibration technique for coupled single-row telemeter and CCD," *3D Digital Imaging and Modeling (3DIM)*; 2005

[2] Q. Zhang and R. Pless, "Extrinsic Calibration of a Camera and Laser Range Finder," *In Proc. International Conference on Intelligent Robots and Systems*; 2004.

[3] D. Scaramuzza, A. Harati and R. Siegwart, "Extrinsic Self Calibration of a Camera and a 3D Laser Range Finder from Natural Scenes," *International Conference on Intelligent Robots and Systems.*; 2007.

[4] A. Lorusso,D. Eggert and R. Fisher, "A comparison of four algorithms for estimating 3-d rigid transformations," *British Machine Vision Conference*; Vol. 1, pp. 237-246; 1995.

[5] C.M. Shakarji, "Least-squares fitting algorithms of the NIST algorithm testing system," *Journal of Research of the National Institute of Standards and Technology*, vol.103, pp. 633-641; 1998.

[6] D.W. Marquardt, "An algorithm for least-squares estimation of non-linear parameters," *Journal of the Society for Industrial and Applied Mathematics* Vol. 11, pp. 431-441; 1963.

[7] P. Gurdjos, J. Kim and I. Kweon, "Geometric and Algebraic Constraints of Projected Concentric Circles and Their Applications to Camera Calibration," *IEEE Trans. Pattern Anal. Mach. Intell.*,Vol. 27, No. 4, pp. 637-642; 2005.

[8] V. Frémont and R. Chellali, "Direct Camera Calibration Using Two Concentric Circles from a Single View," *Proc. Int'l Conf. Artificial Reality and Telexistence*, pp. 93-98; 2002.

[9] K. Kanatani and N. Ohta, "Automatic Detection Of Circular Objects By Ellipse Growing," *International Journal of Image and Graphics*, Vol. 4, pp. 35-50; 2004.

[10] R. Hartley and A. Zisserman, "Multiple view geometry in computer vision," *Cambrige University Press*; 2003.

[11] R. Y. Tsai, "A versatile camera calibration technique for high accuracy 3D machine vision metrology using off-the-shelf TV cameras and lenses," *IEEE J. Robotics Automat.*,Vol. RA-3, No. 4, pp. 323-344; 1987.

[12] Y. Xie and Q. Ji, "A New Efficient Ellipse Detection Method," *International Conference on Pattern Recognition*,Vol. 2, pp. 957-960; 2002.

[13] W. Gander, G. Golub and R. Strebel, "Least-Squares Fitting of Circles and Ellipses," *Technical Report of Computer Science Department, ETH Zürich*; 1994.

[14] K. Arun, T. Huang and S. Blostein, "Least-squares Fitting of Two 3-D Point sets," *IEEE Trans. Pattern Analysis and Machine Intelligence.*,Vol. 9, No. 5, pp. 698-700; 1987.

[15] G. H. Golub and C. Van Loan, "Matrix Computations," *The Johns Hopkins University Press. Third Edition*; 1996.

[16] C. V. Stewart, "Robust Parameter Estimation in Computer Vision," *Society for Industrial and Aplied Mathematics*, Vol. 41, pp. 513-537; 1999.

[17] R. Lupton, "Statistics in Theory and Practice," *Princeton University Press*; 1993.

[18] P. Besl and N. McKay, "A Method for registration of 3-D Shapes," *IEEE Trans. Pattern Analysis and Machine Intelligence*, Vol. 14, No. 2; 1992.

[19] Z. Zhang, "A Flexible New Technique for Camera Calibration," *IEEE Transactions on Pattern Analysis and Machine Intelligence*, Vol. 14, No. 2; 1992.